UCRL-17358

University of California

Ernest O. Lawrence Radiation Laboratory

A MAGNETIC STEERING DEVICE FOR ELECTRON COINCIDENCE EXPERIMENTS

TWO-WEEK LOAN COPY

This is a Library Circulating Copy which may be borrowed for two weeks. For a personal retention copy, call Tech. Info. Division, Ext. 5545

DISCLAIMER

This document was prepared as an account of work sponsored by the United States Government. While this document is believed to contain correct information, neither the United States Government nor any agency thereof, nor the Regents of the University of California, nor any of their employees, makes any warranty, express or implied, or assumes any legal responsibility for the accuracy, completeness, or usefulness of any information, apparatus, product, or process disclosed, or represents that its use would not infringe privately owned rights. Reference herein to any specific commercial product, process, or service by its trade name, trademark, manufacturer, or otherwise, does not necessarily constitute or imply its endorsement, recommendation, or favoring by the United States Government or any agency thereof, or the Regents of the University of California. The views and opinions of authors expressed herein do not necessarily state or reflect those of the United States Government or any agency thereof or the Regents of the University of California.

Submitted to:
Review of Scientific Instruments

UCRL-17358
Preprint

UNIVERSITY OF CALIFORNIA

Lawrence Radiation Laboratory
Berkeley, California

AEC Contract No. W-7405-eng-48

A MAGNETIC STEERING DEVICE FOR ELECTRON COINCIDENCE EXPERIMENTS

R. L. Watson, J. O. Rasmussen, H. R. Bowman and S. G. Thompson

January 27, 1967

A MAGNETIC STEERING DEVICE FOR ELECTRON COINCIDENCE EXPERIMENTS*

R. L. Watson, J. O. Rasmussen, H. R. Bowman and S. G. Thompson

Lawrence Radiation Laboratory
University of California
Berkeley, California

January 27, 1967

I. INTRODUCTION

The suitability and convenience of semiconductor detectors for simultaneous energy measurements of two or more radiations having specific time relationships has led to the increasingly important role of the coincidence method in nuclear spectroscopic investigations. Moreover, with the improved resolution now obtainable, it is now possible to extend coincidence applications to experiments designed to take advantage of the various time relationships existing between electron emission and other nuclear events. Examples of such coincidence relationships include those existing between internal conversion and subsequent X-ray emission, between beta decay and subsequent gamma-ray emission, between alpha decay and the internal conversion of subsequent nuclear transitions, between X-ray emission resulting from K capture and the internal conversion of subsequent nuclear transitions, and between gamma-ray emission and the internal conversion of cascade transitions. The electron coincidence method also lends itself to many other applications such as to the study of internal conversion in coincidence with a nuclear reaction, and to the investigation for which the device to be described in this paper was originally designed--the study of internal conversion in coincidence with nuclear fission.

In all of the above applications, as with any coincidence measurement, a major requirement is the achievement of large total detection efficiencies (intrinsic detector efficiency times detection geometry). Furthermore, it is important that the electrons to be measured are not required to penetrate any quantity of matter (window) so great as to cause a detectable amount of dispersion or energy shift. This restriction requires that the source be located inside the same vacuum chamber

that houses the semiconductor electron detector and hence gives rise to the further problem of shielding the electron detector from interfering radiations (i.e., alpha particles, positrons, X-rays, gamma rays, fission fragments).

We have employed the fringing field of a high gradient electromagnet along with a lithium-drifted silicon detector in a device which overcomes all of the above-mentioned problems in the measurement of electron energies and which may readily be used in conjunction with separate detectors for measuring coincident radiation energies. In this device, electrons are steered away from the source region around a 90 degree circular arc to the detector which is shielded from other radiations emitted at the source.

II. THE MOTION OF AN ELECTRON IN THE STEERING FIELD

The magnetic field used in the steering device is one of rotational symmetry and radial dependence proportional to $1/r^n$. An electron moving in the fringing region of such a field, in general, experiences two types of drift motion--an azimuthal drift around the circumference of the magnet due to the decreasing field strength as a function of distance from the magnet center and a vertical (Z direction) drift consisting of a spiraling motion along the magnetic lines of force.[1] Because the field lines in the fringing field region become highly convergent as they approach the magnet pole tips, the vertical component of the electrons' motion forces it to gyrate in tighter and tighter helical spirals in order to keep its magnetic moment (the ratio of the component of kinetic energy perpendicular to the field lines to the field strength, $T_\perp/H$) a constant.[2] If the field is sufficiently convergent, a point is reached where the parallel (vertical) component of the electrons' kinetic energy becomes zero and the electron is reflected back in the opposite direction. This is the fundamental requirement for a magnetic mirror and it may be shown that the condition for reflection is given by[2]

$$\sin^2 \theta_{crit} \geq H_o/H_R \quad , \qquad (1)$$

where θ_{crit} is the maximum angle between the initial electron trajectory and the field line at the starting point which will result in reflection, H_o is the field strength at the starting point and H_R is the field strength at the reflection point. Hence, for electrons emitted from a source located on the magnet symmetry plane and having vertical kinetic energy components below a critical value, the electron motion is a superposition of a trochoidal motion and a vertical oscillation through the symmetry plane.

The motion of a charged particle in such a field has been studied extensively by Malmfors.[3] Malmfors treated the problem by means of a perturbation method and obtained the following expression for the azimuthal angular displacement of a charged particle after one vertical oscillation through the symmetry plane:

$$\Lambda = \frac{2\pi}{r_o}\frac{mc}{eH_o}\sqrt{E}\sqrt{1+E/2}\left(1 - \frac{n^2-8n+4}{16}\cdot\frac{Z_R^2}{r_o^2} + \ldots\right) \quad . \tag{2}$$

In this equation, r_o is the radial distance from the center of the magnet to the starting point in the plane of symmetry, H_o is the field strength at the starting point, Z_R is the oscillation amplitude (distance from the symmetry plane to point of reflection), and E is the particle energy in units of mc^2. The azimuthal angular displacement of a charged particle after one orbit in the plane of symmetry is given by

$$\Phi = \pi n\frac{\rho_o^2}{r_o^2}\left[1 + \left(\frac{3}{4}n^2+n-1\right)\frac{\rho_o^2}{r_o^2} + \ldots\right] \quad , \tag{3}$$

where ρ_o is the radius of curvature in the plane of symmetry when the oscillation amplitude is zero. Another equation of interest gives the drift time required for a particle to precess 1/4 of the distance around the magnet. It is valid in the region of relativistic velocities and is expressed by

$$\tau = \frac{\pi r_o}{2v_{drift}} = \frac{\pi e}{2mc^2}\frac{H_o r_o^2}{n}\cdot\frac{E+1}{E(1+E/2)}\left(1 + \frac{n(n-2)}{4}\frac{Z_R^2}{r_o^2} + \ldots\right) \quad . \tag{4}$$

An illustration of the region of acceptance into the steering device for a point source located on the symmetry plane is shown in Fig. 1. All electrons emitted between the two cones are transmitted around the magnet.

The transmission of the device may be calculated by integrating the surface area of a sphere over the region bounded by the two escape cones as follows:

$$\Omega = 8 \int_{\frac{\pi}{2} - \Phi}^{\frac{\pi}{2}} \int_{0}^{\frac{\pi}{2}} \sin \theta \, d\theta \, d\varphi = 4\pi \sin \Phi \quad .$$

The total surface area of a sphere is 4π, thus the transmission is given by

$$T = \sin \Phi \quad . \tag{5}$$

Now, from Eq. (1) it follows that

$$\sin^2 \Phi = \cos^2 \theta_c = 1 - \sin^2 \theta_c = 1 - \frac{H_o}{H_R}$$

$$T = \sqrt{1 - \frac{H_o}{H_R}} \quad . \tag{6}$$

Malmfors found that

$$\frac{H_o}{H_R} = \left(1 - \frac{n^2 Z_R{}^2}{2r_o{}^2} + \ldots\right) \tag{7}$$

and substituting the first two terms of this expansion into Eq. (6), the expression for the transmission becomes

$$T = \frac{n}{\sqrt{2}} \frac{Z_{R\,max}}{r_o} \quad . \tag{8}$$

It is seen, then, that the transmission of the steering device is independent of electron energy and is solely determined by the maximum oscillation amplitude of the reflection through the symmetry plane.

III. EXPERIMENTAL DESIGN

The magnetic field used in the steering device is produced by a 100 KVA C-magnet. A plot of the magnetic field strength as a function of radial distance from the center of the magnet is shown in Fig. 2 along with a cross section sketch of the poleface designed to create a nearly constant n fringing field with high convergence at the pole-tips. The radial position of the electron detector and source is also indicated (r_o = 6.5 in.) and the field strength at this radius was 6000 gauss. Since the field strengths at any two radii in a region of constant n are related by the expression

$$\frac{H_1}{H_2} = \frac{r_2^{\,n}}{r_1^{\,n}} \quad , \tag{9}$$

the value of n may be determined from

$$\frac{\log H_2 - \log H_1}{\log r_2 - \log r_1} = -n \quad . \tag{10}$$

The value of n in the region of the detector-source radius was found to be 3.35.

It is of interest, to know the values of several quantities as a function of electron energy: namely, the radius of curvature in the symmetry plane ρ_o, the displacement, d, of an electron after one orbit in the symmetry plane, the maximum displacement, λ, of an electron after one complete vertical oscillation through the symmetry plane, and the time of flight 1/4 of the way around the magnet, τ_{90^o}. The radii of curvature were obtained from a table of magnetic rigidity for electrons[4] while the other quantities were calculated from Eqs. (2), (3) and (4). These quantities are tabulated in Table 1 as a function of electron energy.

A film study of the radial distribution of ^{203}Hg conversion electrons accepted into the steering device was conducted inside a vacuum chamber placed between the polefaces. A strip of X-ray film was mounted inside the vacuum chamber radially from the center of the magnet. The electron source, which consisted of ^{203}Hg amalgamated on

the end of a thin copper wire, was mounted 90° around the magnet at a radial position of 16.5 cm. One of the exposed film strips showing the distribution of electrons transmitted around from the source is presented in Fig. 3 where it is seen that electrons accepted into the device are focused into a narrow band having a width approximately equal to twice the radius of curvature of the electrons in the magnetic field and length determined by the physical dimensions of the system--in this case, the vacuum chamber width.

The transmission of the magnetic steering device is easily calculable from Eq. (8). For our experimental design, (i.e. H_o = 6000 gauss, n = 3.35, r_o = 6.5 in., $Z_{R\ max}$ = 1 in.) the transmission is found from Eq. (8) to be 36.5%. The silicon detector employed as the spectrometer, however, has an active area with a diameter of only 0.53 in. and hence only about 25% of the electrons in the transmitted band actually hit the detector. Furthermore, an appreciable fraction of the electrons which hit the detector suffer backscattering and do not deposit their full energy. By using calibrated ^{109}Cd, ^{203}Hg, ^{207}Bi and ^{137}Cs sources, the total efficiency for electrons transmitted around from the source and detected in the silicon detector was found to be approximately 5% of the total electrons emitted by a source. The efficiency was also found to be nearly constant as a function of energy over the energy range of 0 to 600 keV. (Both the efficiency and its constancy as a function of energy may be seriously affected by the configuration of the source holder as will be discussed in Section IV.)

IV. EXPERIMENTAL APPLICATION

Experiments with standard conversion electron sources disclosed the fact that serious restrictions are placed on the configuration of the source holder as a result of the trajectories imposed upon the electrons by the magnetic steering device. Specifically, these restrictions stem from the following two properties of the electron trajectories in the steering field:

(a) The electron drift displacement, d, in the azimuthal direction (around the magnet) after one orbit, is so small the electrons tend to reenter the source backing;

(b) The small wavelength of the oscillation through the symmetry plane, λ, causes electrons having low energies or low takeoff angles to collide with the source holder.

Both of these effects cause serious tailing and peak displacement in measured electron spectra. It was found, however, that these problems could be minimized by employing carefully designed source holders and backings.

The source arrangement found to work best consisted of a circular wire loop 1/4 in. in diameter constructed from 1/64 in. diameter stainless steel wire. A straight 5/8 in. length of stainless steel wire of the same diameter is soldered perpendicular to the loop plane at a point along the periphery and used to connect the loop to a micrometer probe attached to the vacuum chamber. The source backing is mounted over the loop and the source deposited in the center. For our electron sources, the backings consist of a 2 $\mu g/cm^2$ film of zapon enveloped over both sides of the source loop with approximately 10 $\mu g/cm^2$ of gold vaporized on each side over the zapon giving a total source backing thickness of about 24 $\mu g/cm^2$. The electron sources are usually prepared by evaporating to dryness small drops of the source solutions placed at the centers of the films.

As an example of the quality of the measurements we are able to obtain with the magnetic steering device, a spectrum of the internal conversion electrons arising from the decay of ^{203}Hg is shown in Fig. 4 taken with a lithium-drifted silicon detector (3 mm depletion depth) in the steering device. The detector was operated at an optimum tem-

perature of -93°C and 318 volts bias, and incorporated a field effect transistor cooled to -135°C in the input stage of the preamplifier.[5] The measured resolution was 3.0 keV for the K line of ^{203}Hg as shown in Fig. 4 where the L and M lines and a shoulder due to the N line may also be seen. The electron peaks display some tailing, but this is felt to be mostly due to the thickness of the source rather than interference from the source holder and backing.

A sketch of the basic layout used in our studies of internal conversion electrons in coincidence with nuclear fission is presented in Fig. 5.[6] As indicated, electrons starting at the symmetry plane precess in trochoidal orbits around the magnet in a 90° arc to the electron detector while being reflected from poleface to poleface along magnetic lines of force. (The trajectory of an electron leaving at the critical reflection angle θ_c is depicted.) The fission fragment detectors were placed parallel to the symmetry plane and only those electrons which were emitted near 90° with respect to the fragment detector axis were allowed to reach the electron detector. A large lead shield was located in a position which blocked any interfering radiation. A very useful application was made of the fact that the transmission of the steering device can be controlled by varying the maximum oscillation amplitude ($Z_{R\ max}$). This property was employed, as illustrated in Fig. 6 by moving the fission source off the symmetry plane and restricting the region of acceptance into the steering device by means of two deflectors. These two deflectors limited the maximum oscillation amplitude of the electrons and since the acceptance angle of the device is proportional to the maximum oscillation amplitude as depicted for electrons emitted at point 1 and point 2 in Fig. 6, this restriction required that the fission fragments from which the electrons were emitted be near the symmetry plane at the time of emission. The transmission at any point between the deflectors may be calculated from Eq. (6) by replacing H_o with the magnetic field intensity at the source position. From Eq. (7), it is found that

$$\frac{H_s}{H_R} = \frac{H_o}{H_R} \times \frac{H_s}{H_o} = \frac{\left(1 - \frac{n^2}{2}\frac{Z_R^2}{r_o^2}\right)}{\left(1 - \frac{n^2}{2}\frac{Z_s^2}{r_o^2}\right)} , \qquad (11)$$

where Z_s is the distance from the symmetry plane to the point of emission. It follows, after substitution of this expression into Eq. (6), that the transmission at any point between the deflectors is given by

$$T(z) = n\sqrt{\frac{Z_{R\,max}^{2} - Z_s^{2}}{2r_o^{2} - n^{2} Z_s^{2}}} \quad . \tag{12}$$

The deflectors were spaced 2 cm apart in the experiments and hence $Z_{R\,max}$ was 1 cm.

The calculated detection efficiency as a function of the distance of the fragment from the symmetry plane at the time of electron emission (Z_s) is plotted in Fig. 7. It is seen that by positioning the deflectors 2 cm apart, a time resolution of approximately 1.7 nsec was achieved since the average fission fragment velocity is about 1 cm/nsec. In this way it was possible to measure half-lives of transitions in the nanosecond range.

V. CONCLUSION

The magnetic steering device described in this paper should prove quite useful in many aspects of semiconductor electron spectroscopy. Although the device is particularly attractive for the coincidence applications suggested here because of the high detection efficiency it offers, it could be used to equal advantage in any experiment where it is required to obtain electron spectra in the presence of other interfering radiations. It is well suited, for example, to application in an internal conversion coefficient spectrometer where it is desired to measure simultaneously the conversion electron and gamma-ray spectra of a nuclide. Without a means of shielding the electron detector, the low-energy portion of the electron spectrum is usually obscured by X-rays and Compton electrons created by the gamma rays impinging upon the electron detector. The half-life application of the device might also be useful in the study of nuclear reaction products and alpha recoil nuclides.

FOOTNOTE AND REFERENCES

* This work was performed under the auspices of the U. S. Atomic Energy Commission.

1. A. Simon, An Introduction to Thermonuclear Research, Pergamon Press, New York, 1959, p. 35.
2. J. R. Reitz and F. J. Milford, Foundations of Electromagnetic Theory, Addison-Wesley Publishing Co., Reading, Mass., 1960, p. 276.
3. K. G. Malmfors, Arkiv För Fysik, 13 (1958), p. 237.
4. F. W. Breivogel and M. D. Holtz, Table of Kinetic Energy vs. Magnetic Rigidity for Electrons, UCRL-10494, (1962).
5. E. Elad, Nucl. Instr. Methods 37, 327 (1965).
6. R. L. Watson, H. R. Bowman, S. G. Thompson, and J. O. Rasmussen, Internal Conversion Processes, J. H. Hamilton, editor, Academic Press, Inc., New York (1966), p. 423.

FIGURE CAPTIONS

Fig. 1. An illustration of the region of acceptance into the magnetic steering device for electrons emitted from a point source located on the symmetry plane. All electrons emitted between the two cones are transmitted around the magnet to the electron detector.

Fig. 2. Magnetic field profile and sketch of poleface cross section.

Fig. 3. A film strip which was exposed at the detector position to electrons transmitted around the magnet from the source position in the steering device.

Fig. 4. Spectrum of the internal conversion electrons associated with the 279.1 keV gamma-ray transition in ^{203}Tl taken with a lithium-drifted silicon detector in the magnetic steering device.

Fig. 5. A diagram depicting the magnetic steering mechanism for an electron emitted at the critical reflection angle θ_{crit}. The electron starts at the symmetry plane and precesses in trochoidal orbits around the magnet in a 90° arc to the detector while being reflected from poleface to poleface along magnetic lines of force.

Fig. 6. A diagram of the fragment detector-source-deflector assembly. With the source positioned as shown, only those electrons which were emitted while the fragment was between the two deflectors could be detected. The limitation imposed upon the electron trajectories by the deflectors caused the critical angle of acceptance for electrons to vary from 0° at the deflector position to a maximum of 8° at the symmetry plane (position 1).

Fig. 7. The calculated detection efficiency for electrons emitted from fission fragments as a function of the distance of the fragment from the symmetry plane at the time of emission.

Table 1. Calculated quantities pertaining to the motion of electrons in the magnetic steering device. (6000 gauss, n = 3.35, r_o = 6.5 in.)

Energy (keV)	ρ_o (cm)	d (cm)	λ (cm)	$\tau_{(90^o)}$ (nsec)
10.0	.056	.002	.250	772.8
50.0	.129	.011	.569	160.2
100.0	.186	.022	.824	83.4
150.0	.233	.035	1.031	57.6
200.0	.275	.048	1.216	44.5
250.0	.313	.063	1.387	36.6
300.0	.350	.078	1.549	31.3
350.0	.385	.095	1.704	27.4
400.0	.419	.112	1.855	24.5
450.0	.452	.131	2.002	22.2
500.0	.485	.150	2.145	20.3
550.0	.517	.170	2.287	18.8
600.0	.548	.192	2.426	17.5
650.0	.580	.214	2.564	16.4
700.0	.610	.238	2.700	15.4
750.0	.641	.262	2.835	14.5
800.0	.671	.287	2.969	13.8
850.0	.701	.314	3.102	13.1
900.0	.731	.341	3.234	12.5
950.0	.761	.369	3.366	11.9
1000.0	.791	.399	3.497	11.4

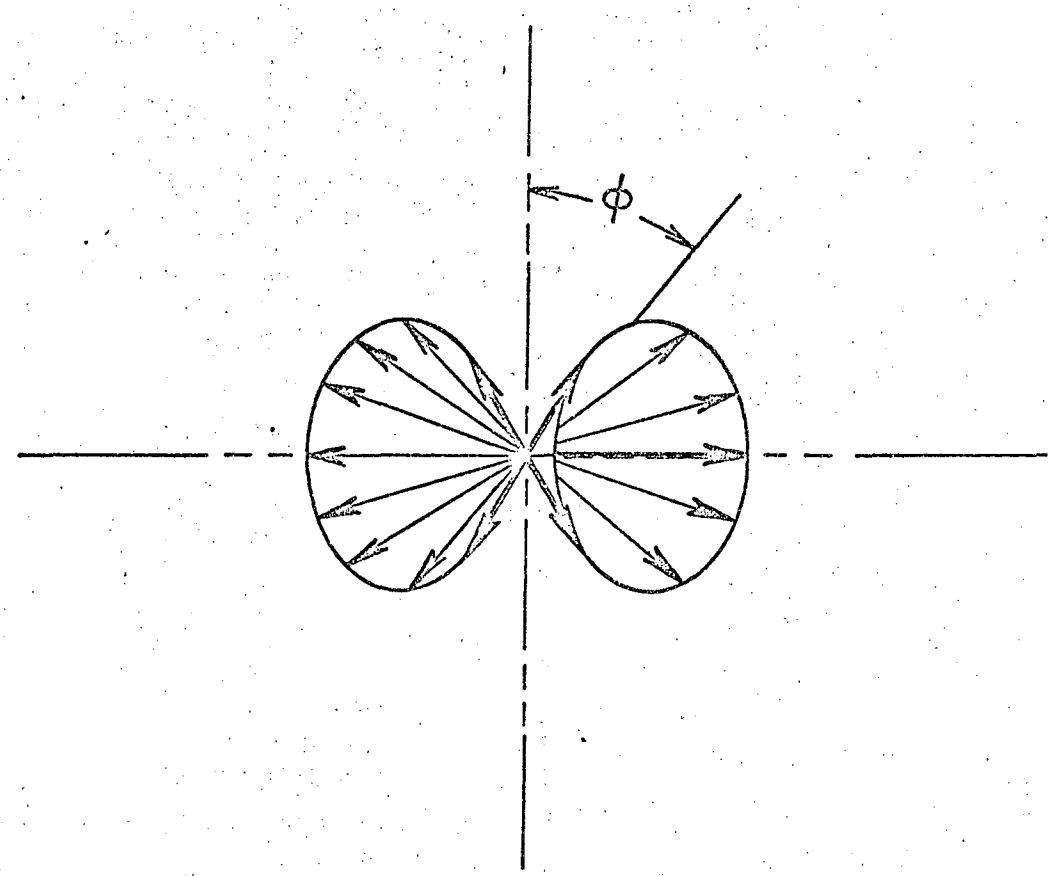

MUB-9749

Fig. 1.

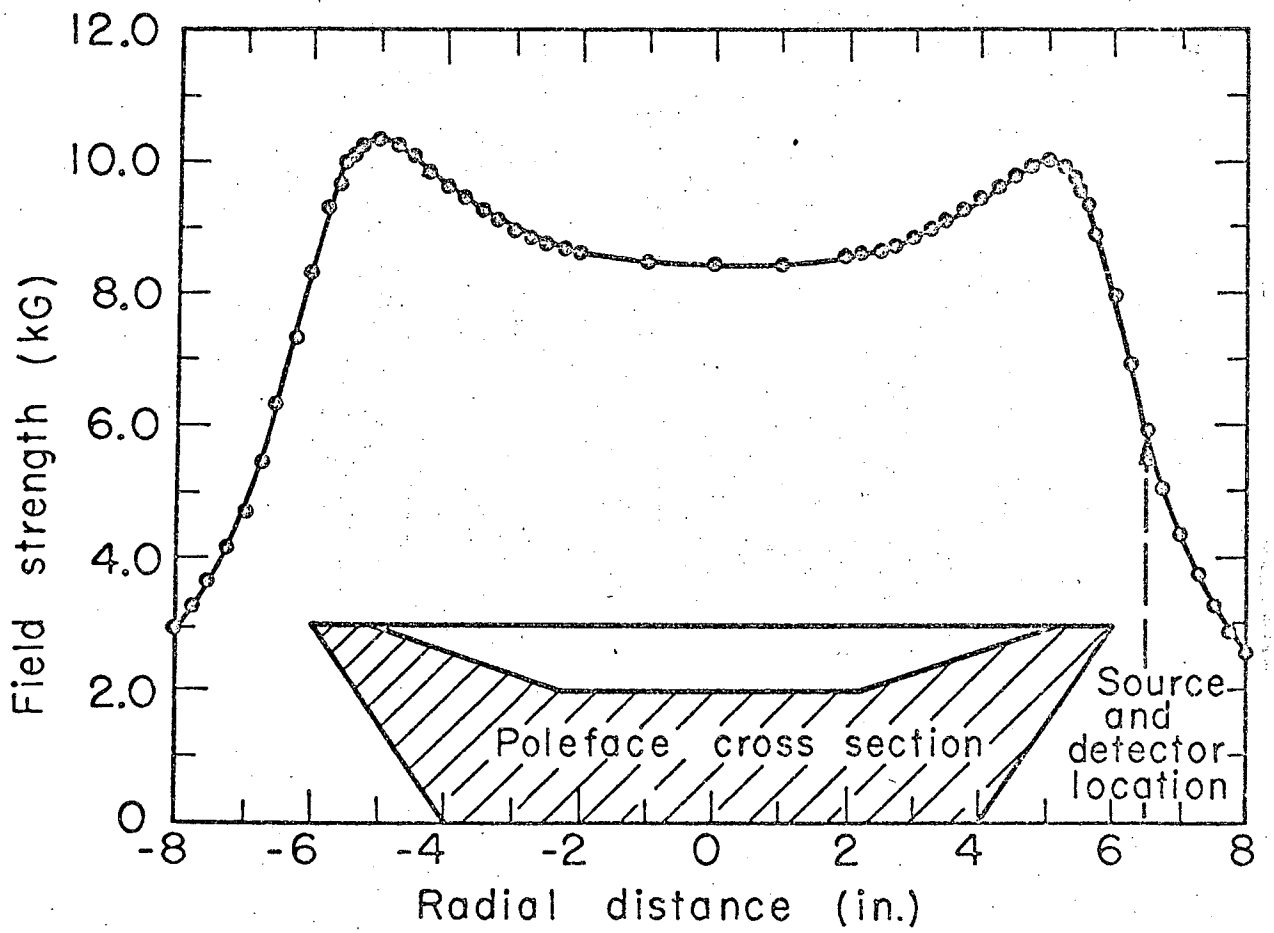

MUB-10882

Fig. 2.

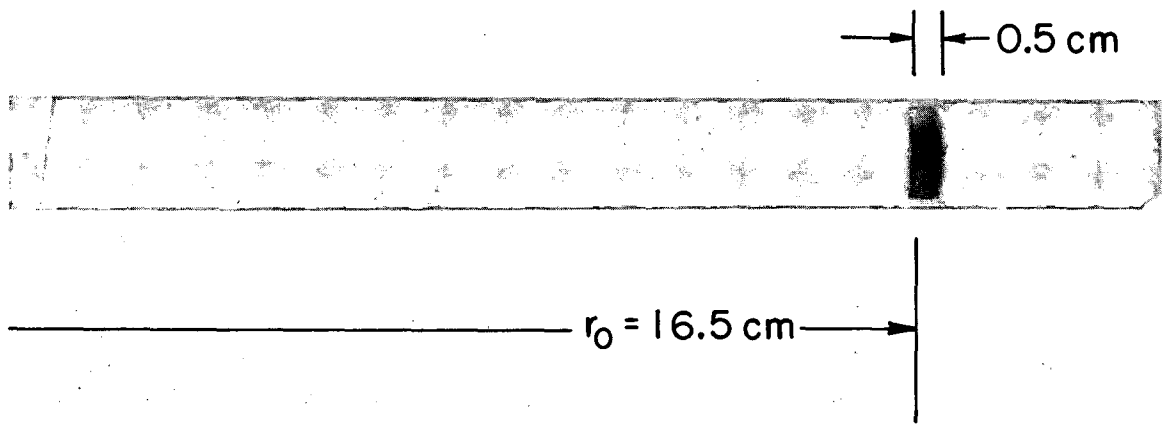

BBH 672-71

Fig. 3.

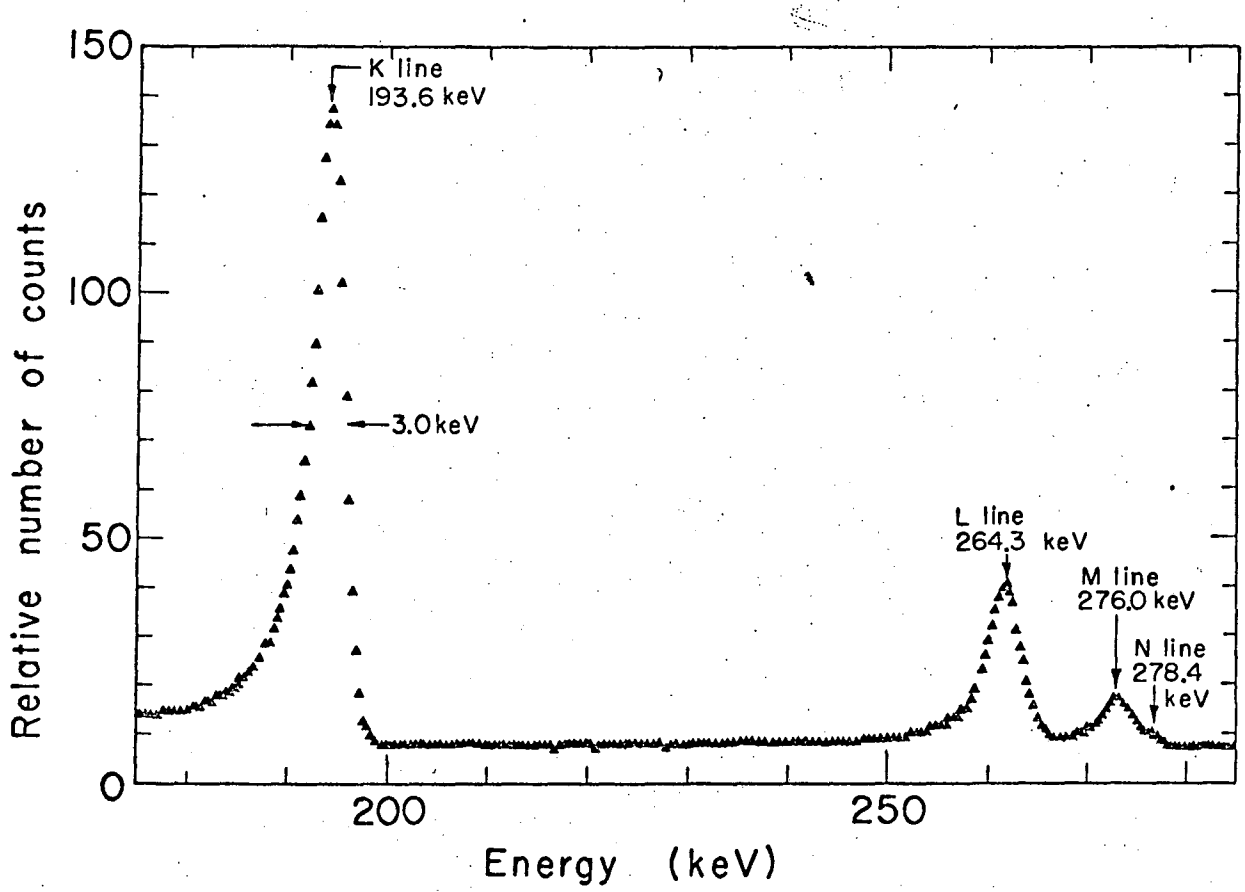

MUB-10852

Fig. 4.

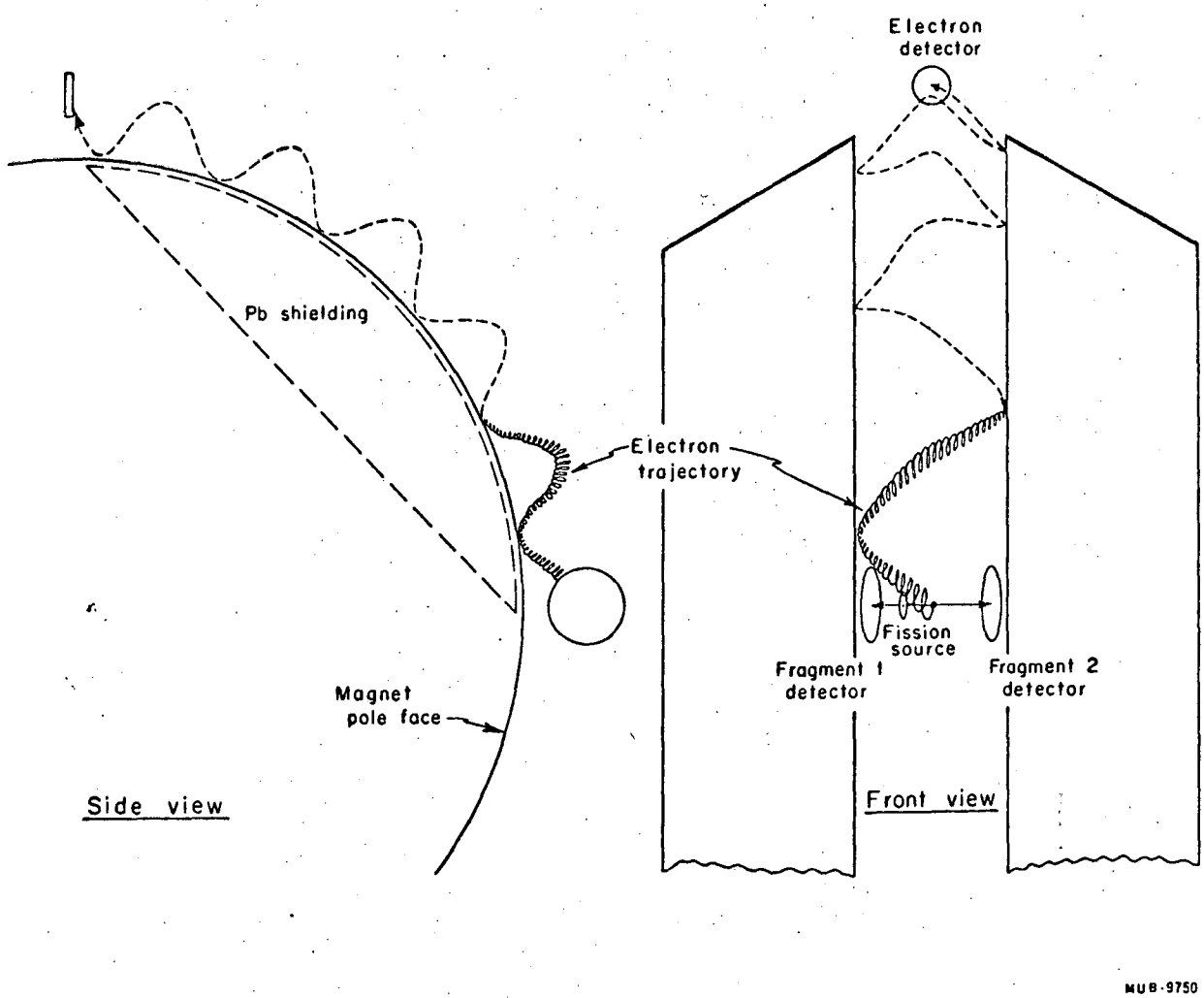
Electron detector
Pb shielding
Electron trajectory
Fission source
Fragment 1 detector
Fragment 2 detector
Magnet pole face
Side view
Front view
MUB-9750

Fig. 5.

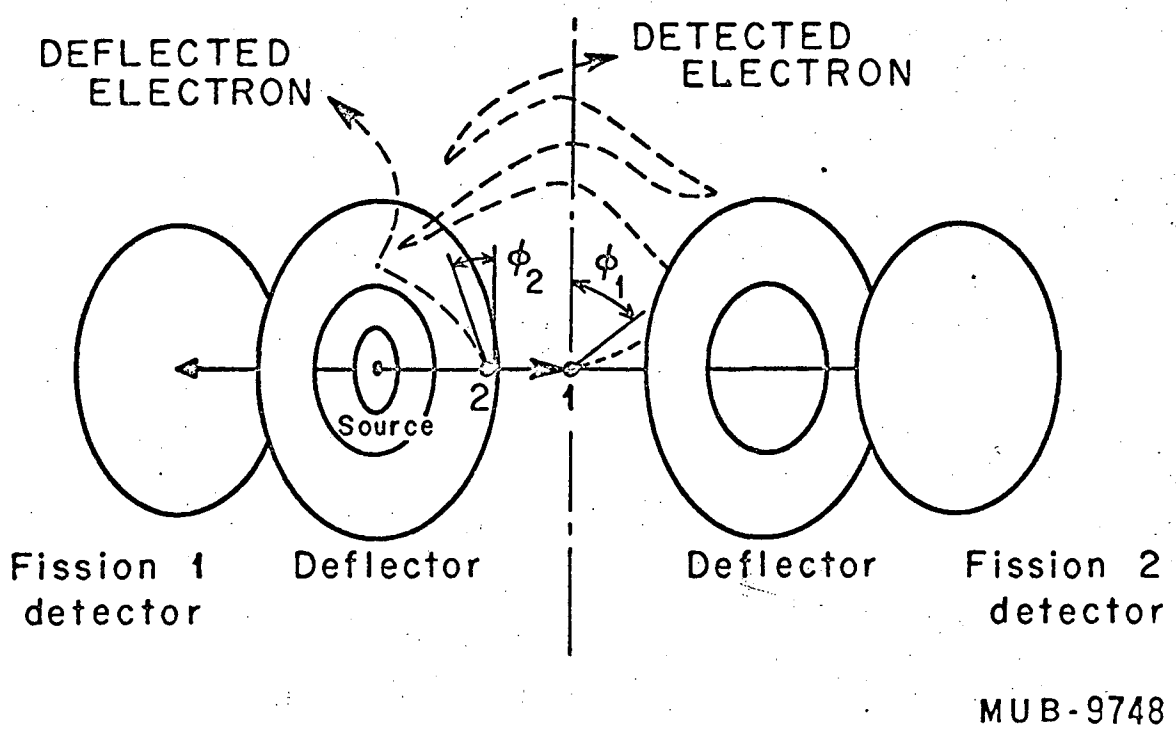
DEFLECTED ELECTRON
DETECTED ELECTRON
ϕ_2
ϕ_1
2
1
Source
Fission 1 detector
Deflector
Deflector
Fission 2 detector
MUB-9748

Fig. 6.

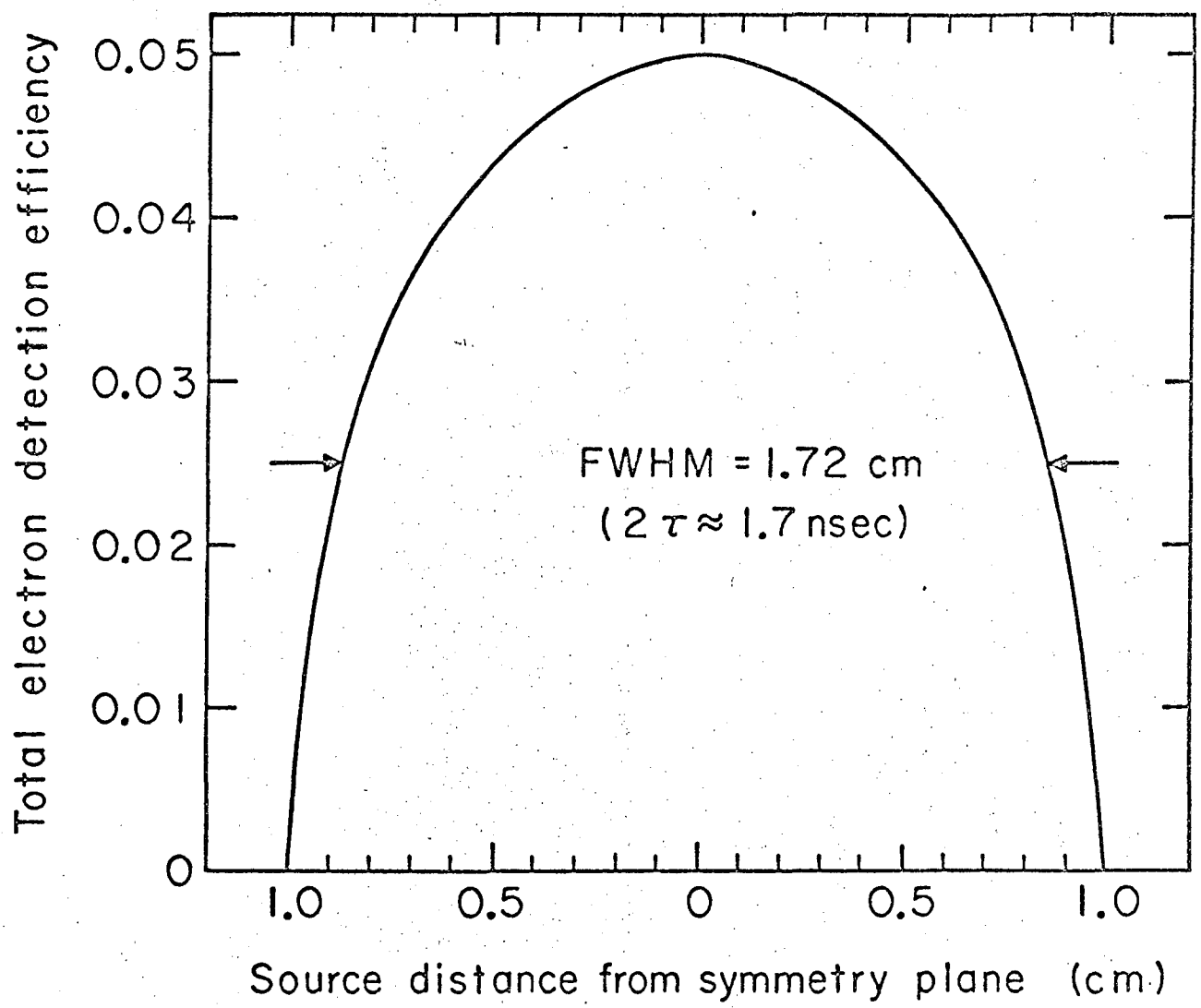

MUB-9904

Fig. 7.

This report was prepared as an account of Government sponsored work. Neither the United States, nor the Commission, nor any person acting on behalf of the Commission:

A. Makes any warranty or representation, expressed or implied, with respect to the accuracy, completeness, or usefulness of the information contained in this report, or that the use of any information, apparatus, method, or process disclosed in this report may not infringe privately owned rights; or

B. Assumes any liabilities with respect to the use of, or for damages resulting from the use of any information, apparatus, method, or process disclosed in this report.

As used in the above, "person acting on behalf of the Commission" includes any employee or contractor of the Commission, or employee of such contractor, to the extent that such employee or contractor of the Commission, or employee of such contractor prepares, disseminates, or provides access to, any information pursuant to his employment or contract with the Commission, or his employment with such contractor.